Iron promotes oxidative cell death caused by bisretinoids of retina

Keiko Ueda[a], Hye Jin Kim[a], Jin Zhao[a], Ying Song[b], Joshua L. Dunaief[b], and Janet R. Sparrow[a,c,1]

[a]Department of Ophthalmology, Columbia University Medical Center, New York, NY 10032; [b]F. M. Kirby Center for Molecular Ophthalmology, Scheie Eye Institute, University of Pennsylvania, Philadelphia, PA 19104; and [c]Department of Pathology and Cell Biology, Columbia University Medical Center, New York, NY 10032

Intracellular Fe plays a key role in redox active energy and electron transfer. We sought to understand how Fe levels impact the retina, given that retinal pigment epithelial (RPE) cells are also challenged by accumulations of vitamin A aldehyde adducts (bisretinoid lipofuscin) that photogenerate reactive oxygen species and photodecompose into damaging aldehyde- and dicarbonyl-bearing species. In mice treated with the Fe chelator deferiprone (DFP), intracellular Fe levels, as reflected in transferrin receptor mRNA expression, were reduced. DFP-treated albino $Abca4^{-/-}$ and agouti wild-type mice exhibited elevated bisretinoid levels as measured by high-performance liquid chromatography or noninvasively by quantitative fundus autofluorescence. Thinning of the outer nuclear layer, a parameter indicative of the loss of photoreceptor cell viability, was also reduced in DFP-treated albino $Abca4^{-/-}$. In contrast to the effects of the Fe chelator, mice burdened with increased intracellular Fe in RPE due to deficiency in the Fe export proteins hephaestin and ceruloplasmin, presented with reduced bisretinoid levels. These findings indicate that intracellular Fe promotes bisretinoid oxidation and degradation. This interpretation was supported by experiments showing that DFP decreased the oxidative/degradation of the bisretinoid A2E in the presence of light and reduced cell death in cell-based experiments. Moreover, light-independent oxidation and degradation of A2E by Fenton chemistry products were evidenced by the consumption of A2E, release of dicarbonyls, and generation of oxidized A2E species in cell-free assays.

bisretinoid | lipofuscin | iron | retinal pigment epithelium | macular degeneration

While Fe is required for many metabolic processes, it is also a redox-active metal capable of causing molecular and cellular dysfunction by catalyzing the formation of hydroxyl free radical (OH•) via the Fenton reaction (1). Accordingly, several mechanisms operate to regulate Fe import, storage, and export to prevent Fe overload or deficiency (1). Most nonheme Fe is bound to transferrin in the circulation. For access to the retina, Fe-laden transferrin binds to the transferrin receptor on the basolateral surface of retinal pigment epithelial (RPE) cells and the apical surface of retinal vascular endothelial cells. Both of these surfaces face the blood supply. Within RPE cells, Fe dissociates from transferrin to enter a cytosolic pool of labile Fe that can be utilized, stored, or exported. Intracellular Fe can be stored in ferritin, a multisubunit protein consisting of heavy (H) and light (L) chains. Ferroportin exports ferrous (Fe^{2+}) Fe that is not utilized or stored. Since only ferric (Fe^{3+}) Fe can be accepted by transferrin in the circulation, ferroportin coordinates with ferroxidases such as ceruloplasmin (Cp), or hephaestin (Heph) within the plasma membrane, to oxidize Fe from the ferrous Fe^{2+} (four unpaired electrons) to ferric Fe^{3+} (five unpaired electrons) form. This conversion is also protective since oxidation of Fe from Fe^{2+} to Fe^{3+} prevents Fe^{2+}-mediated oxidative damage by means of hydroxyl free radical generation (Fenton reaction).

Fe excess or dysregulation in the eye is toxic to photoreceptors and RPE when introduced to the vitreous by a foreign object (for example, in patients with siderosis), or when it accumulates in the RPE in aceruloplasminemia due to mutations in the Fe exporter ceruloplasmin (2, 3). RPE cells are also a target of retinopathy associated with β-thalassemia, an autosomal recessive hemoglobinopathy requiring blood transfusions for survival (4). Fe accumulates in RPE with age-related macular degeneration (AMD) (5, 6).

RPE cells are unusual in that they are subjected to an age-related accumulation of photoreactive vitamin A aldehyde-derived compounds (7–11). This family of fluorophores, only one of which is A2E, has bisretinoid structures and constitutes the lipofuscin of RPE. The structure common to all of these fluorophores is a conjugated system of double bonds along each of two side arms that terminate in β-ionone rings. The polyene structures on the long arms of the fluorophore generate absorbances in the visible range of the spectrum (12) and allow for both electron and energy transfer. The molecular and cell damage mediated by these compounds is attributable, at least in some measure, to their propensity to photogenerate reactive oxygen species and to photodegrade into aldehyde- and dicarbonyl-bearing fragments (13, 14). Some of these photodegradation products are the dicarbonyls methylglyoxal (MG) and glyoxal (GO) (13, 14) that modify proteins and are known to populate subretinal drusen (15, 16). This bisretinoid photodegradative process is responsible for the lower bisretinoid levels

Significance

Cells are subject to metabolic sources of oxidizing species and to the need to regulate Fe, a redox-active metal. Retinal pigment epithelial (RPE) cells have to contend with an additional, unique source of oxidative stress: photooxidative insult from bisretinoids that accumulate as lipofuscin. Here we report that Fe can interact with bisretinoids in RPE to promote cell damage. These findings inform disease processes in both Fe-related and bisretinoid-associated retinal degeneration. The link between Fe and bisretinoid oxidation also highlights opportunities for repurposed and combination therapies. This could include visual cycle inhibitors as a treatment for maculopathy associated with elevated retinal Fe, and Fe chelation to aid in suppressing the damaging effects of bisretinoids in juvenile and age-related macular degeneration.
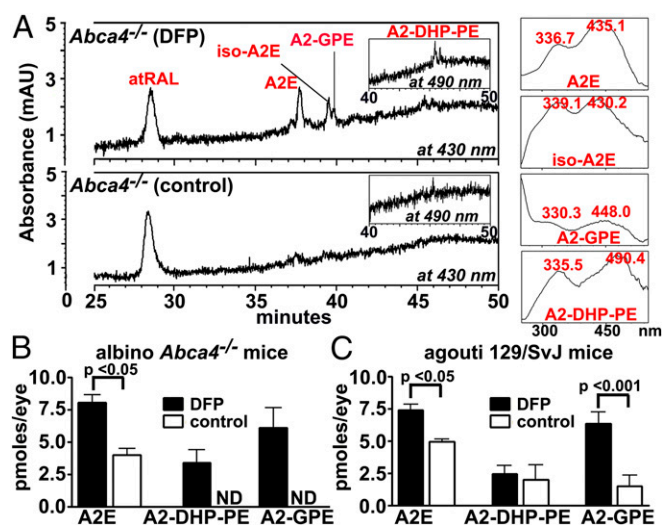
MEDICAL SCIENCES

Fig. 1. The bisretinoids A2E, A2-GPE, and A2-DHP-PE in mice treated with the Fe chelator DFP. Oral DFP was administered from age 2 to 6 mo. (*A*) Representative reverse phase HPLC chromatographs illustrating the detection of all *trans*-retinal (atRAL), A2E (Rt 37.6 m), iso-A2E (Rt 39.4 m), A2-GPE (Rt 39.8 m), and A2-DHP-PE (Rt 45.3 m). (*Insets* at *Right*) UV-visible spectra of chromatographic peaks corresponding to A2E (all-*trans*-A2E), iso-A2E (C13/14 *cis*-A2E), A2-GPE, and A2-DHP-PE. (*B* and *C*) Chromatographic quantitation of bisretinoids in albino *Abca4*$^{-/-}$ and agouti 129 wild-type mice. A2E (the sum of all-*trans*-A2E and iso-A2E) and A2-DHP-PE were quantified by HPLC. A2-GPE was quantified by UPLC. Values are means ± SEM; four eyes (two mice) or six eyes (three mice) were pooled for each sample of DFP-treated or control albino *Abca4*$^{-/-}$ mice, and eight eyes (four mice) were pooled for agouti 129Sv mice. *P* values were determined by one-way ANOVA and Sidak's multiple comparison test. Rt, retention time.

measured in albino versus black mice and in light- versus dark-reared mice (17) and may explain why early and intermediate AMD are associated with lower fundus autofluorescence intensity [measured as quantitative fundus autofluorescence (qAF)] in central retina (18). There is evidence that this photodegradative process is also ongoing in human retina. For instance, photo-oxidation and photodegradation can explain the RPE lipofuscin fluorescence bleaching that occurs in nonhuman primates during in vivo fluorescence imaging (19, 20). Similar fluorescence bleaching probably also accounts for the hyperautofluorescent lines coursing parallel to retinal blood vessels that are sometimes visible in fundus AF images when the position of vessels relative to RPE has changed after surgical repair of retinal detachment (21, 22). In the latter case, it is possible that under the shadow of

a blood vessel, lipofuscin photobleaching is reduced and thus a vessel imprint of more intense autofluorescence is revealed upon retinal translocation.

Our initial observation that the FDA-approved Fe chelator deferiprone (DFP) when delivered to mice, altered bisretinoid levels in retina, led us to consider whether the oxidative processes enabled by intracellular Fe accentuates bisretinoid oxidation and degradation. Thus, we embarked on a plan to examine the combined effects of Fe and bisretinoid on oxidative insult to RPE and photoreceptor cells.

Results

Quantitation of Bisretinoids in DFP-Treated Mice by High-Performance Liquid Chromatography. The Fe chelator DFP is moderately lipophilic, cell permeable, and has been shown in mice to reduce intracellular Fe burden in retina without evidence of retinal toxicity (23–26). We delivered DFP to wild-type agouti 129/SvJ mice and to albino *Abca4*$^{-/-}$ mice from age 2–6 mo. The *Abca4* null mutant mouse is well known to accumulate bisretinoid fluorophores such as A2E and A2-GPE at elevated rates (27–30). In the DFP-treated albino *Abca4*$^{-/-}$ mice, A2E/iso-A2E were present in amounts that were twofold higher ($P < 0.05$) than in control untreated mice (difference as percentage of control) (Fig. 1). A2E levels in the DFP-treated agouti wild-type mice were 49% higher than in untreated mice ($P < 0.05$). This treatment effect can be explained as a DFP-mediated reduction in the degradative loss of bisretinoid. Since photodegradation of bisretinoid is more pronounced in the albino eye (17), high-performance liquid chromatography (HPLC)-quantified bisretinoid was not appreciably different in albino *Abca4*$^{-/-}$ versus agouti *Abca4*$^{+/+}$ mice (Fig. 1 *B* and *C*).

Measuring Fundus Autofluorescence in DFP-Treated Mice by qAF. We also measured bisretinoid noninvasively using a previously published in vivo qAF approach (31, 32). Analysis revealed 26% higher levels of fundus autofluorescence in albino *Abca4*$^{-/-}$ mice treated with DFP from age 2–4 mo ($P > 0.05$) and 56% increased qAF in the mice treated from 2 to 6 mo of age ($P < 0.05$) (Fig. 2). The higher qAF in DFP-treated compared with untreated mice is indicative of reduced bisretinoid loss due to oxidation. The difference between DFP-treated and control mice when measured by qAF is less than when measured by HPLC. We attribute this to the greater baseline short-wavelength fundus autofluorescence (SW-AF) signal recorded in albino mice due to the more pronounced intraocular light.

Measuring Retinal Fe Levels Through Transferrin Receptor qPCR. When cells need more Fe, transferrin receptor mRNA is stabilized, leading to more Fe uptake (33). Transferrin receptor
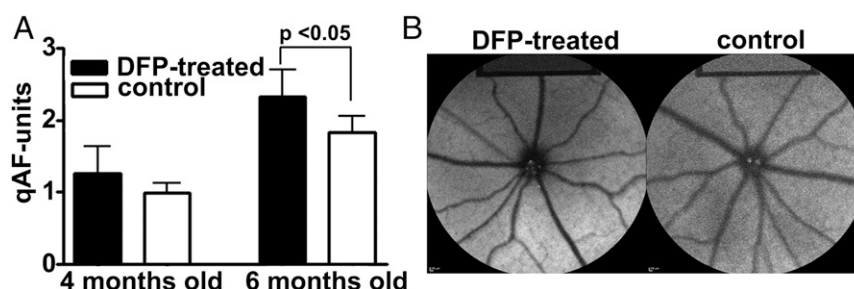
Fig. 2. Quantitative fundus autofluorescence (qAF) (488 nm) in *Abca4*$^{-/-}$ albino mice aged 4 and 6 mo. Mice were treated with DFP beginning at 2 mo of age. (*A*) qAF increases in DFP-treated mice. Values are means ± SEM, eight or nine mice per group. *P* value was determined by one-way ANOVA and Sidak's multiple comparison test. (*B*) Short-wavelength fundus autofluorescence images acquired for qAF analysis. Note that in the two images, the fundus appears to present with similar gray levels; however, the internal reference at the *Top* of the image of the DFP-treated mouse is darker, indicating higher fundus AF (qAF) levels.

Fig. 3. Effect of DFP on ocular transferrin receptor expression in $Abca4^{-/-}$ albino mice. Transferrin receptor mRNA is increased in neural retina (age 4 mo) and RPE/choroid/sclera (age 4 and 6 mo) in DFP-treated mice beginning at age 2 mo. Each value is the mean of four eyes analyzed from two mice. P values were derived by one-way ANOVA and Sidak's multiple comparison test.

mRNA levels reflect intracellular Fe concentrations (23, 34), since in cells needing more Fe, transferrin receptor mRNA is stabilized. In $Abca4^{-/-}$ mice receiving DFP in drinking water from age 2 mo, transferrin receptor mRNA levels, quantified in neural retina by qRT-PCR (35) were 1.73-fold greater than controls ($P < 0.05$) at 4 mo of age, while the fold change in RPE/choroid/sclera was 1.66 ($P < 0.05$) (Fig. 3).

Outer Nuclear Layer Thickness. In albino $Abca4^{-/-}$ mice, the accelerated formation of bisretinoid leads to reduced photoreceptor cell viability that is detected at age 8 mo by measuring the thickness of the outer nuclear layer (ONL) (31, 36). In the DFP-treated mice, thinning of the ONL was less pronounced (Fig. 4). Interobserver agreement was calculated according to Bland and Altman (37). The mean difference between two observers (bias) was 0.05 μm and the 95% limits of agreement was −1.8–1.7 μm. The ONL area, determined using the s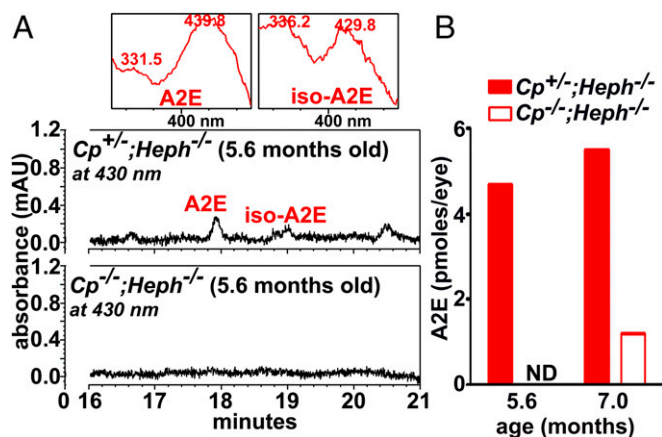um of ONL thicknesses in superior and inferior retina (0.2–2 mm), was increased by 25% ($P < 0.001$, unpaired two-tailed t test) in superior hemiretina of mice receiving oral DFP and 17% ($P < 0.001$) in inferior hemiretina compared with the control mice.

$Cp^{-/-}$; $Heph^{-/-}$ Mice. Cp and its homolog Heph are copper-containing ferroxidase proteins that convert Fe^{2+} to Fe^{3+} so as to enable cellular Fe export. Accordingly, deficiency in Heph and Cp leads to elevated intracellular Fe in RPE (38). We found that $Cp^{-/-}$; $Heph^{-/-}$ mice also exhibited reduced bisretinoid measured as A2E/iso-A2E (Fig. 5). We interpret this finding as indicative of increased A2E oxidation and degradation due to elevated Fe.

In Vitro Mechanistic Experiments. The higher levels of bisretinoid and qAF in DFP-treated mice (Figs. 1 and 2) are consistent with a mechanism involving a reduction in oxidation-associated degradation of bisretinoid in the presence of Fe chelation. Support for the latter mechanism was forthcoming in experiments employing a human RPE cell line (ARPE-19) that had accumulated A2E and was irradiated with 430 nm light (Fig. 6). Loss of A2E due to oxidation and degradation was diminished in cells pretreated with DFP before light exposure (Fig. 6A). Moreover, the corresponding loss of cell viability that is associated with these conditions was reduced with DFP pretreatment (Fig. 6B). Since H_2O_2 in the presence of Fe^{2+} (Fenton reaction) also generates highly reactive hydroxyl radical (OH•), we tested light-independent effects of these Fenton chemistry reactants on A2E. Exposure of A2E to $FeSO_4$ and H_2O_2 degraded A2E with concomitant release of MG and GO that were detected by trapping with 2,4-dinitrophenylhydrazine (DNPH) (Fig. 7 A and B) (Fig. S1). Moreover, DFP reduced the production of MG and GO by Fenton chemistry, suppressed the degradative loss of A2E and reduced the formation of oxidized forms of A2E (Fig. 7 B and C).

Discussion

Here in $Abca4^{-/-}$ mice treated with the Fe chelator DFP, we observed an increase in HPLC quantified bisretinoid and higher fundus AF intensity measured as qAF. Conversely, elevated Fe in RPE of $Cp^{-/-}$; $Heph^{-/-}$ mice (39) resulted in decreased bisretinoids. These findings indicate that Fe can promote the oxidation-based degradation of bisretinoid. This interpretation is further supported by ancillary in vitro data showing that DFP protected against degradative loss of A2E in the presence of light, while Fe and H_2O_2 promoted the degradation of A2E. The DFP-associated protection against ONL thinning also indicates that the process of Fe-promoted bisretinoid oxidation-associated degradation contributes to photoreceptor cell loss in $ABCA4$-related disease. These findings are consistent with our previous observation that the antioxidant activity of vitamin E conserved levels of RPE bisretinoid by suppressing photooxidation (17), the

Fig. 4. Outer nuclear layer (ONL) thickness in 8-mo-old $Abca4^{-/-}$ albino mice. (A) ONL (mean ± SEM) in DFP-treated (n, 14) and control (n, 11) mice are plotted as distance from optic nerve head (ONH). (B) ONL areas calculated from ONL thickness measurements acquired 0.2–2.0 mm from the ONH in superior and inferior hemiretinae. P values were determined by one-way ANOVA and Sidak's multiple comparison test.

Fig. 5. UPLC quantitation of A2E and iso-A2E in mice deficient in ceruloplasmin (Cp) and hephaestin (Heph) ($Cp^{-/-}$; $Heph^{-/-}$) and $Cp^{+/-}$; $Heph^{-/-}$ mice. (*A*) Detection of A2E and iso-A2E in $Cp^{+/-}$; $Heph^{-/-}$ and $Cp^{-/-}$; $Heph^{-/-}$ mice. (*Insets at Top*) UV-visible spectra of chromatographic peaks corresponding to A2E (all-*trans*-A2E) and iso-A2E (C13/14 *cis*-A2E). (*B*) Picomoles per eye were calculated using calibration curves constructed from authentic standards. ND, not detected. Values based on single samples, four to eight eyes per sample.

higher levels of RPE bisretinoid being evidenced by quantitative HPLC and qAF. Measurement of outer nuclear layer thickness also revealed photoreceptor cell protection in the vitamin E-treated $Abca4^{-/-}$ mice. Since photodegradation of bisretinoid is more pronounced in albino versus pigmented mice, HPLC-quantified bisretinoid is more abundant in pigmented mice (17) (Fig. 1).

We have previously demonstrated that lipofuscin bisretinoids can be consumed by the processes of photooxidation and photodegradation even in ambient lighting (17). Bisretinoids are prone to oxidation because of their conjugated systems of double bonds (e.g., C-C = C-C = C). The oxidation of bisretinoids can proceed by multiple independent mechanisms (10, 40, 41). For instance, using A2E as a model it has been shown that bisretinoids are visible light photosensitizers that generate singlet oxygen by energy transfer, and superoxide anion by donation of an electron to ground state molecular O_2 (10, 40–42). As with some other photosensitizers (43), A2E can also serve as the substrate for reaction (oxidation) with singlet oxygen and radical oxygen species at double bonds (10, 44). Thus, the side arms of A2E are subsequently oxidized by a molecular singlet oxygen-mediated pathway that adds two oxygen atoms to form a cyclic peroxide (*m/z* 624) (10, 13, 42, 45). Alternatively addition of one oxygen atom can also occur so as to form epoxide and furanoid moieties (44, 46). Here the produced superoxide anion can generate H_2O_2 by dismutation [spontaneously or superoxide dismutase (SOD)-catalyzed] followed by the highly reactive hydroxyl radical (OH•) that is generated from H_2O_2 with Fe as catalyst. The OH• radical is a powerful oxidant because of its unpaired electron (47, 48). Accordingly, OH• can readily break carbon double bonds, especially the conjugated double bonds like those that form the side arms of bisretinoids. This reactivity is significant, given the present findings indicating that in the absence of light, the OH• radical can also oxidize A2E.

Oxidative degradation of bisretinoids such as A2E and all-*trans*-retinal dimer, releases a mixture of aldehyde- and dicarbonyl-bearing fragments (MG and GO) that elicit cellular damage. Since it has been reported that reaction of MG with L-arginine can be catalyzed by Fe (particularly Fe^{2+}) (49), Fe may also promote the modification of proteins by bisretinoid photofragments. Electron donors produced by light exposure such as superoxide anion (O_2^-) or cellular reductants such as glutathione (GSH) or ascorbate, both of which are abundant in the retina,

can recycle Fe^{3+} to Fe^{2+}, enabling Fe to act catalytically even when Fe availability is low.

The retina is subject to photochemical damage that is readily demonstrable by exposure to light for prolonged periods or at heightened intensities (50, 51). Efforts to understand the molecular mechanisms of light damage have identified both Fe (52) and bisretinoids (53) as participants. In the latter case, we found that light damage-associated ONL thinning and dropout of RPE nuclei were more pronounced in $Abca4^{-/-}$ mice having elevated levels of RPE bisretinoid than in age-matched wild-type mice. The ONL thinning was also greater in 5-mo-old versus 2-mo-old mice. In $Rpe65^{rd12}$ mice bisretinoids are not detected chromatographically and light damage was not observed (53). Systemic administration of the Fe chelator and antioxidant lipoic acid (alpha-lipoic acid) or DFP protects against light-induced photoreceptor degeneration in the mouse retina (34, 54). DFP, when administered orally to mice (1 mg/mL, 5 mg/d) has been shown to protect against retinal degeneration when the latter is induced by RPE Fe accumulation in *Cp/Heph* double KO (DKO) mice (55), by sodium iodate-mediated oxidative damage to RPE cells or by the rd6 mutation (24).

Fe and bisretinoids may also have links to AMD. The benefits afforded to patients with AMD by antioxidant intake indicate that oxidative mechanisms are an important factor contributing to AMD pathogenesis (56, 57). It is thus significant that Fe and bisretinoid initiate separate, but perhaps overlapping toxic oxidative processes (49, 58, 59). Perls' staining revealed that Fe levels were increased in AMD-affected maculas compared with healthy age-matched maculas (5) particularly in the RPE and Bruch's membrane of early AMD, geographic atrophy, and patients with exudative AMD. Examination of the postmortem macula of a 72-y-old white male with geographic atrophy revealed Fe overload in the RPE and photoreceptor cell layers along with ferritin and ferroportin in the photoreceptor cells and internal limiting membrane. Conversely, healthy maculas were only weakly labeled with anti-ferritin and anti-ferroportin antibody (60). Transferrin is also up-regulated in AMD (61). Proteins modified by dicarbonyls are detected in sub-RPE drusen (15, 16) and these dicarbonyls are the same as those released by photodegradation of bisretinoids such as A2E and all-*trans*-retinal dimer. These findings indicate a possible link between photodegradation of RPE lipofuscin and sub-RPE changes that confer risk of AMD. Evidence that bisretinoid lipofuscin and Fe can initiate damaging light-mediated mechanisms (described above) is supported by epidemiological studies pointing to a relationship between AMD risk and sunlight exposure (62–69).
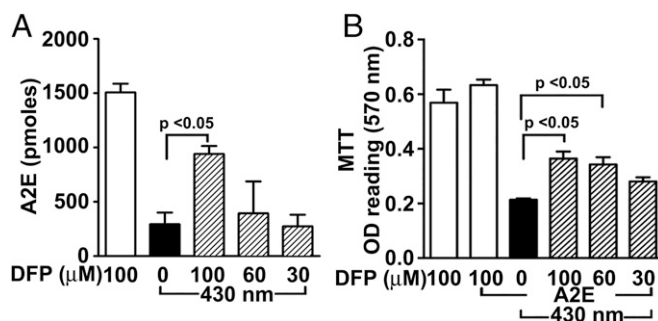

Fig. 6. Effects of DFP in the presence of bisretinoid photooxidation: cellular assays. ARPE-19 cells that have accumulated A2E were treated with DFP (30, 60, and 100 μM, 30 min) and then illuminated at 430 nm. (*A*) The Fe chelator DFP reduces photooxidative loss of A2E in ARPE-19 cells (HPLC analysis). (*B*) The reduced cell viability associated with A2E photooxidation was attenuated by pretreatment with the Fe chelator DFP. *P* values were determined by one-way ANOVA and Tukey's multiple comparison test.
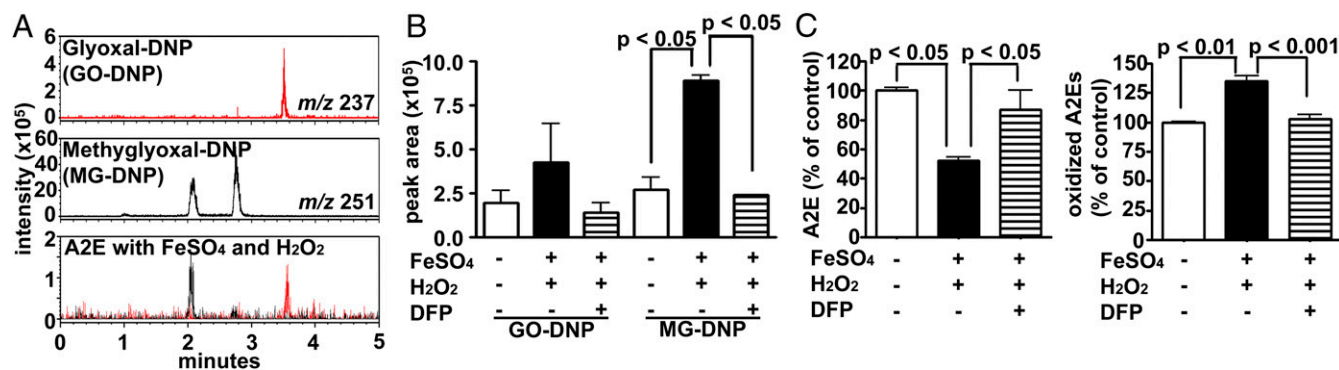
Fig. 7. Fenton reaction products oxidize and degrade A2E. Detection of dicarbonyl compounds and oxidized A2E species. (*A*) UPLC-MS detection of authentic glyoxal-DNP (GO-DNP; Rt 3.5 m) (red) and two isomers of methylglyoxal-DNP (MG-DNP; Rt 2.1, 2.5 m) (black) and DNP-derivatized products generated when A2E was incubated with $FeSO_4$ and H_2O_2. MS-selected ion monitoring chromatograms at m/z 237 and 251 [M-H]$^-$. (*B*) Quantitation of dicarbonyls in ion monitoring chromatograms. Values are means ± SEM, two independent experiments; *P* values were determined by one-way ANOVA and Sidak's multiple comparison test. (*C*) HPLC quantitation of the consumption of A2E (*Left*) and formation of oxidized A2E species (*Right*) in the presence of $FeSO_4$ and H_2O_2. Values are means ± SEM of two independent experiments; *P* values were determined by one-way ANOVA and Tukey's multiple comparison test. Rt, retention time.

These findings point to opportunities for drug repurposing and combination therapies. For instance, Fe chelation alone or in combination with inhibitors of bisretinoid formation (70) could serve as a unique therapy for recessive Stargardt disease (STGD1), a bisretinoid-related disease, and possibly AMD. Conversely, drugs that suppress the synthesis and toxic activities of bisretinoid could be beneficial for Fe-related conditions such as siderosis retinopathy.

Methods

Mouse Models. Albino *Abca4*$^{-/-}$, agouti 129S1/SvImJ mice and mice deficient in ceruloplasmin and hephaestin (*Cp*$^{-/-}$; *Heph*$^{-/-}$) (38) were studied. Mice received DFP (Ferriprox) (Barr Pharma, pharmaceutical grade) in drinking water (1 mg/mL) from age 2 mo to age 4 or 6 mo. The intake of DFP was ∼3–5 mg per day. Animal protocols were approved by the Institutional Animal Care and Use Committee of Columbia University. Details are provided in *Supporting Information*.

Quantitative HPLC and Ultra Performance Liquid Chromatography. Mouse eyecups (4–8 eyes per sample as indicated) were homogenized, extracted in chloroform/methanol (2:1), and analyzed for bisretinoid by reversed-phase HPLC (A2E, iso-A2E) using an Alliance System (Waters Corp.) or Waters Acquity Ultra Performance Liquid Chromatography (UPLC)-MS System (A2E and iso-A2E in X-bridge, A2-GPE in phenyl) (Waters) as described (17, 29). Molar quantities per eye were calculated by comparison with synthesized standards. The pyridinium bisretinoid A2E and its *cis* isomer, iso-A2E, were measured separately and summed (A2E/iso-A2E). To

detect DNP-derivatized dicarbonyl, incubated samples were extracted and analyzed by UPLC-MS (71).

qAF. Images were acquired and analyzed as previously described (31).

Cell and Cell-Free Assays. ARPE-19 cells that had accumulated A2E (71) were treated with the Fe chelator DFP (30–100 μM) and then irradiated (430 ± 30 nm) for 30 min. A2E was then extracted and quantified by HPLC (17). Cytotoxicity was measured by the MTT (4,5-dimethylthiazol-2-yl)-2,5-diphenyltetrazolium bromide) colorimetric assay (Roche Diagnostics Corporation) (72). Synthesized A2E (9) (50 μM in distilled water with 0.5% DMSO) was incubated with $FeSO_4$ (200 μM), H_2O_2 (500 μM), and DFP (600 μM) for 3 h at 37 °C and peak areas were quantified by UPLC (73).

Measurement of ONL Thickness. Sagittal sections traversing the optic nerve head were analyzed and the ONL area was calculated (36).

qRT-PCR for Transferrin Receptor Expression. Neural retina was separated from RPE/choroid/sclera, total RNA was isolated using Qiagen RNeasy Plus Micro kit (Qiagen), and reverse transcription was performed (Reverse Transcription kit; Thermo Fisher Scientific) (23, 34). Real-time PCR was performed with Applied Biosystems 7900HT. Probes and primers were as follows: transferrin receptor, Mm00441941_m1; 18s rRNA internal control, Hs99999901_s1.

1. Halliwell B, Gutteridge JMC (2015) *Free Radicals in Biology and Medicine* (Oxford Univ Press, Oxford), 5th Ed.
2. Dunaief JL, et al. (2005) Macular degeneration in a patient with aceruloplasminemia, a disease associated with retinal iron overload. *Ophthalmology* 112:1062–1065.
3. Wolkow N, et al. (2011) Aceruloplasminemia: Retinal histopathologic manifestations and iron-mediated melanosome degradation. *Arch Ophthalmol* 129:1466–1474.
4. Bhoiwala DL, Dunaief JL (2016) Retinal abnormalities in β-thalassemia major. *Surv Ophthalmol* 61:33–50.
5. Hahn P, Milam AH, Dunaief JL (2003) Maculas affected by age-related macular degeneration contain increased chelatable iron in the retinal pigment epithelium and Bruch's membrane. *Arch Ophthalmol* 121:1099–1105.
6. Biesemeier A, Yoeruek E, Eibl O, Schraermeyer U (2015) Iron accumulation in Bruch's membrane and melanosomes of donor eyes with age-related macular degeneration. *Exp Eye Res* 137:39–49.
7. Eldred GE, Katz ML (1988) Fluorophores of the human retinal pigment epithelium: Separation and spectral characterization. *Exp Eye Res* 47:71–86.
8. Dorey CK, Wu G, Ebenstein D, Garsd A, Weiter JJ (1989) Cell loss in the aging retina. Relationship to lipofuscin accumulation and macular degeneration. *Invest Ophthalmol Vis Sci* 30:1691–1699.
9. Parish CA, Hashimoto M, Nakanishi K, Dillon J, Sparrow J (1998) Isolation and one-step preparation of A2E and iso-A2E, fluorophores from human retinal pigment epithelium. *Proc Natl Acad Sci USA* 95:14609–14613.
10. Ben-Shabat S, et al. (2002) Formation of a nonaoxirane from A2E, a lipofuscin fluorophore related to macular degeneration, and evidence of singlet oxygen involvement. *Angew Chem Int Ed Engl* 41:814–817.
11. Liu J, Itagaki Y, Ben-Shabat S, Nakanishi K, Sparrow JR (2000) The biosynthesis of A2E, a fluorophore of aging retina, involves the formation of the precursor, A2-PE, in the photoreceptor outer segment membrane. *J Biol Chem* 275:29354–29360.
12. Kim SR, Jang YP, Sparrow JR (2010) Photooxidation of RPE lipofuscin bisretinoids enhances fluorescence intensity. *Vision Res* 50:729–736.
13. Wu Y, Yanase E, Feng X, Siegel MM, Sparrow JR (2010) Structural characterization of bisretinoid A2E photocleavage products and implications for age-related macular degeneration. *Proc Natl Acad Sci USA* 107:7275–7280.
14. Yoon KD, Yamamoto K, Ueda K, Zhou J, Sparrow JR (2012) A novel source of methylglyoxal and glyoxal in retina: Implications for age-related macular degeneration. *PLoS One* 7:e41309.
15. Handa JT, et al. (1999) Increase in the advanced glycation end product pentosidine in Bruch's membrane with age. *Invest Ophthalmol Vis Sci* 40:775–779.
16. Crabb JW, et al. (2002) Drusen proteome analysis: An approach to the etiology of age-related macular degeneration. *Proc Natl Acad Sci USA* 99:14682–14687.
17. Ueda K, Zhao J, Kim HJ, Sparrow JR (2016) Photodegradation of retinal bisretinoids in mouse models and implications for macular degeneration. *Proc Natl Acad Sci USA* 113:6904–6909.
18. Gliem M, et al. (2016) Quantitative fundus autofluorescence in early and intermediate age-related macular degeneration. *JAMA Ophthalmol* 134:817–824.

19. Morgan JI, Dubra A, Wolfe R, Merigan WH, Williams DR (2009) In vivo auto-fluorescence imaging of the human and macaque retinal pigment epithelial cell mosaic. *Invest Ophthalmol Vis Sci* 50:1350–1359.

20. Morgan JI, et al. (2008) Light-induced retinal changes observed with high-resolution autofluorescence imaging of the retinal pigment epithelium. *Invest Ophthalmol Vis Sci* 49:3715–3729.

21. Pandya VB, Ho IV, Hunyor AP (2012) Does unintentional macular translocation after retinal detachment repair influence visual outcome? *Clin Experiment Ophthalmol* 40:88–92.

22. Shiragami C, et al. (2010) Unintentional displacement of the retina after standard vitrectomy for rhegmatogenous retinal detachment. *Ophthalmology* 117:86–92.e1.

23. Hadziahmetovic M, et al. (2011) The oral iron chelator deferiprone protects against iron overload-induced retinal degeneration. *Invest Ophthalmol Vis Sci* 52:959–968.

24. Hadziahmetovic M, et al. (2012) The oral iron chelator deferiprone protects against retinal degeneration induced through diverse mechanisms. *Transl Vis Sci Technol* 1:7.

25. Song D, et al. (2014) The oral iron chelator deferiprone protects against systemic iron overload-induced retinal degeneration in hepcidin knockout mice. *Invest Ophthalmol Vis Sci* 55:4525–4532.

26. Song D, Dunaief JL (2013) Retinal iron homeostasis in health and disease. *Front Aging Neurosci* 5:24.

27. Radu RA, et al. (2008) Accelerated accumulation of lipofuscin pigments in the RPE of a mouse model for ABCA4-mediated retinal dystrophies following Vitamin A supplementation. *Invest Ophthalmol Vis Sci* 49:3821–3829.

28. Weng J, et al. (1999) Insights into the function of Rim protein in photoreceptors and etiology of Stargardt's disease from the phenotype in abcr knockout mice. *Cell* 98:13–23.

29. Yamamoto K, Yoon KD, Ueda K, Hashimoto M, Sparrow JR (2011) A novel bisretinoid of retina is an adduct on glycerophosphoethanolamine. *Invest Ophthalmol Vis Sci* 52:9084–9090.

30. Kim SR, et al. (2007) The all-trans-retinal dimer series of lipofuscin pigments in retinal pigment epithelial cells in a recessive Stargardt disease model. *Proc Natl Acad Sci USA* 104:19273–19278.

31. Sparrow JR, et al. (2013) Quantitative fundus autofluorescence in mice: Correlation with HPLC quantitation of RPE lipofuscin and measurement of retina outer nuclear layer thickness. *Invest Ophthalmol Vis Sci* 54:2812–2820.

32. Flynn E, Ueda K, Auran E, Sullivan JM, Sparrow JR (2014) Fundus autofluorescence and photoreceptor cell rosettes in mouse models. *Invest Ophthalmol Vis Sci* 55:5643–5652.

33. He X, et al. (2007) Iron homeostasis and toxicity in retinal degeneration. *Prog Retin Eye Res* 26:649–673.

34. Hadziahmetovic M, et al. (2012) Microarray analysis of murine retinal light damage reveals changes in iron regulatory, complement, and antioxidant genes in the neurosensory retina and isolated RPE. *Invest Ophthalmol Vis Sci* 53:5231–5241.

35. Chen P, et al. (2001) A photic visual cycle of rhodopsin regeneration is dependent on Rgr. *Nat Genet* 28:256–260.

36. Wu L, Nagasaki T, Sparrow JR (2010) Photoreceptor cell degeneration in Abcr $^{(-/-)}$ mice. *Adv Exp Med Biol* 664:533–539.

37. Bland JM, Altman DG (1986) Statistical methods for assessing agreement between two methods of clinical measurement. *Lancet* 1:307–310.

38. Hahn P, et al. (2004) Disruption of ceruloplasmin and hephaestin in mice causes retinal iron overload and retinal degeneration with features of age-related macular degeneration. *Proc Natl Acad Sci USA* 101:13850–13855.

39. Wolkow N, et al. (2012) Ferroxidase hephaestin's cell-autonomous role in the retinal pigment epithelium. *Am J Pathol* 180:1614–1624.

40. Pawlak A, et al. (2003) Comparison of the aerobic photoreactivity of A2E with its precursor retinal. *Photochem Photobiol* 77:253–258.

41. Gaillard ER, et al. (2004) A mechanistic study of the photooxidation of A2E, a component of human retinal lipofuscin. *Exp Eye Res* 79:313–319.

42. Sparrow JR, et al. (2002) Involvement of oxidative mechanisms in blue-light-induced damage to A2E-laden RPE. *Invest Ophthalmol Vis Sci* 43:1222–1227.

43. Bonnett R, Martinez G (2001) Photobleaching of sensitisers used in photodynamic therapy. *Tetrahedron* 57:9513–9547.

44. Jang YP, Matsuda H, Itagaki Y, Nakanishi K, Sparrow JR (2005) Characterization of peroxy-A2E and furan-A2E photooxidation products and detection in human and mouse retinal pigment epithelial cell lipofuscin. *J Biol Chem* 280:39732–39739.

45. Sparrow JR, et al. (2003) A2E-epoxides damage DNA in retinal pigment epithelial cells. Vitamin E and other antioxidants inhibit A2E-epoxide formation. *J Biol Chem* 278:18207–18213.

46. Dillon J, Wang Z, Avalle LB, Gaillard ER (2004) The photochemical oxidation of A2E results in the formation of a 5,8,5′,8′-bis-furanoid oxide. *Exp Eye Res* 79:537–542.

47. Stephenson NA, Bell AT (2007) Mechanistic insights into iron porphyrin-catalyzed olefin epoxidation by hydrogen peroxide: Factors controlling activity and selectivity. *J Mol Catal A Chem* 275:54–62.

48. Gelalcha FG, Bitterlich B, Anilkumar G, Tse MK, Beller M (2007) Iron-catalyzed asymmetric epoxidation of aromatic alkenes using hydrogen peroxide. *Angew Chem Int Ed Engl* 46:7293–7296.

49. Wittmann I, et al. (2001) Role of iron in the interaction of red blood cells with methylglyoxal. Modification of L-arginine by methylglyoxal is catalyzed by iron redox cycling. *Chem Biol Interact* 138:171–187.

50. Hunter JJ, et al. (2012) The susceptibility of the retina to photochemical damage from visible light. *Prog Retin Eye Res* 31:28–42.

51. Organisciak DT, Vaughan DK (2010) Retinal light damage: Mechanisms and protection. *Prog Retin Eye Res* 29:113–134.

52. Chen L, et al. (2003) Increased expression of ceruloplasmin in the retina following photic injury. *Mol Vis* 9:151–158.

53. Wu L, Ueda K, Nagasaki T, Sparrow JR (2014) Light damage in Abca4 and Rpe65rd12 mice. *Invest Ophthalmol Vis Sci* 55:1910–1918.

54. Zhao L, et al. (2014) Systemic administration of the antioxidant/iron chelator α-lipoic acid protects against light-induced photoreceptor degeneration in the mouse retina. *Invest Ophthalmol Vis Sci* 55:5979–5988.

55. Greferath U, Guymer RH, Vessey KA, Brassington K, Fletcher EL (2016) Correlation of histologic features with in vivo imaging of reticular pseudodrusen. *Ophthalmology* 123:1320–1331.

56. Fritsche LG, et al. (2013) Seven new loci associated with age-related macular degeneration. *Nat Genet* 45:433–439, 439e1–2.

57. Handa JT (2012) How does the macula protect itself from oxidative stress? *Mol Aspects Med* 33:418–435.

58. Zhou J, Gao X, Cai B, Sparrow JR (2006) Indirect antioxidant protection against photooxidative processes initiated in retinal pigment epithelial cells by a lipofuscin pigment. *Rejuvenation Res* 9:256–263.

59. Jang YP, Zhou J, Nakanishi K, Sparrow JR (2005) Anthocyanins protect against A2E photooxidation and membrane permeabilization in retinal pigment epithelial cells. *Photochem Photobiol* 81:529–536.

60. Dentchev T, Hahn P, Dunaief JL (2005) Strong labeling for iron and the iron-handling proteins ferritin and ferroportin in the photoreceptor layer in age-related macular degeneration. *Arch Ophthalmol* 123:1745–1746.

61. Chowers I, et al. (2006) The iron carrier transferrin is upregulated in retinas from patients with age-related macular degeneration. *Invest Ophthalmol Vis Sci* 47:2135–2140.

62. Cruickshanks KJ, Klein R, Klein BEK (1993) Sunlight and age-related macular degeneration. The Beaver Dam Eye study. *Arch Ophthalmol* 111:514–518.

63. Tomany SC, Cruickshanks KJ, Klein R, Klein BEK, Knudtson MD (2004) Sunlight and the 10-year incidence of age-related maculopathy: The Beaver Dam Eye study. *Arch Ophthalmol* 122:750–757.

64. Cruickshanks KJ, Klein R, Klein BEK, Nondahl DM (2001) Sunlight and the 5-year incidence of early age-related maculopathy: The beaver dam eye study. *Arch Ophthalmol* 119:246–250.

65. Klein BE, et al. (2014) Sunlight exposure, pigmentation, and incident age-related macular degeneration. *Invest Ophthalmol Vis Sci* 55:5855–5861.

66. Huang EJ, et al. (2014) Prevalence and risk factors for age-related macular degeneration in the elderly Chinese population in south-western Taiwan: The Puzih eye study. *Eye (Lond)* 28:705–714.

67. Schick T, et al. (2016) History of sunlight exposure is a risk factor for age-related macular degeneration. *Retina* 36:787–790.

68. Fletcher AE, et al. (2008) Sunlight exposure, antioxidants, and age-related macular degeneration. *Arch Ophthalmol* 126:1396–1403.

69. Sui GY, et al. (2013) Is sunlight exposure a risk factor for age-related macular degeneration? A systematic review and meta-analysis. *Br J Ophthalmol* 97:389–394.

70. Sparrow JR (2016) Vitamin A-aldehyde adducts: AMD risk and targeted therapeutics. *Proc Natl Acad Sci USA* 113:4564–4569.

71. Zhou J, Ueda K, Zhao J, Sparrow JR (2015) Correlations between photodegradation of bisretinoid constituents of retina and dicarbonyl-adduct deposition. *J Biol Chem* 290:27215–27227.

72. Zhao J, Kim HJ, Sparrow JR (2017) Multimodal fundus imaging of sodium iodate-treated mice informs RPE susceptibility and origins of increased fundus autofluorescence. *Invest Ophthalmol Vis Sci* 58:2152–2159.

73. Sparrow JR, et al. (2012) The bisretinoids of retinal pigment epithelium. *Prog Retin Eye Res* 31:121–135.